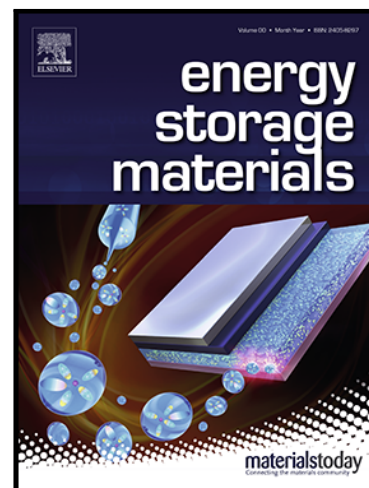


Journal Pre-proof

Quantitatively Regulating Defects of 2D Tungsten Selenide to Enhance Catalytic Ability for Polysulfide Conversion in a Lithium Sulfur Battery

Hao-Jie Li , Kai Xi , Wei Wang , Sheng Liu , Guo-Ran Li ,
Xue-Ping Gao

PII: S2405-8297(21)00541-9
DOI: <https://doi.org/10.1016/j.ensm.2021.11.024>
Reference: ENSM 1933



To appear in: *Energy Storage Materials*

Received date: 18 September 2021
Revised date: 5 November 2021
Accepted date: 14 November 2021

Please cite this article as: Hao-Jie Li , Kai Xi , Wei Wang , Sheng Liu , Guo-Ran Li , Xue-Ping Gao , Quantitatively Regulating Defects of 2D Tungsten Selenide to Enhance Catalytic Ability for Polysulfide Conversion in a Lithium Sulfur Battery, *Energy Storage Materials* (2021), doi: <https://doi.org/10.1016/j.ensm.2021.11.024>

This is a PDF file of an article that has undergone enhancements after acceptance, such as the addition of a cover page and metadata, and formatting for readability, but it is not yet the definitive version of record. This version will undergo additional copyediting, typesetting and review before it is published in its final form, but we are providing this version to give early visibility of the article. Please note that, during the production process, errors may be discovered which could affect the content, and all legal disclaimers that apply to the journal pertain.

© 2021 Elsevier B.V. All rights reserved.

Quantitatively Regulating Defects of 2D Tungsten Selenide to Enhance Catalytic Ability for Polysulfide Conversion in a Lithium Sulfur Battery

Hao-Jie Li^a, Kai Xi^b, Wei Wang^a, Sheng Liu^a, Guo-Ran Li^{a*}, and Xue-Ping Gao^a

^a*Institute of New Energy Material Chemistry, School of Materials Science and Engineering, Renewable Energy Conversion and Storage Center, Nankai University, Tianjin 300350, China*

^b*Department of Engineering, University of Cambridge, Cambridge CB3 0FA, United Kingdom*

* Corresponding author.

E-mail: guoranli@nankai.edu.cn.

Highlights

- On the basal planes of 2D WSe₂, defects are quantitatively created.
- The relationship among the defects of the 2D material, catalytic ability, and electrochemical performance of lithium sulfur battery are clearly established.
- The optimal S/WSe_{1.51}/CNT electrode delivers a high areal capacity of 11.3 mAh cm⁻², and outstanding cycle stability with a decay rate of 0.025% during 1000 cycles at 1C rate.
- The effect mechanism of the defects on lithium sulfur battery is revealed deeply.

Abstract

Introducing defects into 2D materials can increase the coordinatively unsaturated sites that are usually also catalytically active sites. How does the level of defects influence catalytic performance and how to take advantage of defects to optimize the 2D materials? In this work, anionic Se vacancies and edge dislocations are regulated in 2D WSe₂ as a model of transition metal dichalcogenide host material for the sulfur cathode. The defective 2D WSe₂ with different W/Se ratios are quantitatively investigated the influence of the defects on enhancing the cathodic process in lithium sulfur (Li-S) batteries. With a moderate level of defects, WSe_{1.51} shows the optimal performance for adsorbing polysulfides, catalysing polysulfides conversion, and promoting liquid-solid transformation, all of which are crucial steps for Li-S battery. The corresponding sulfur cathode delivers a high initial areal capacity of 11.3 mAh cm⁻², and excellent cycle stability with a decay rate of 0.025% during 1000 cycles at 1C rate.

Even in a pouch cell, the excellent cyclability and flexibility are still available. The results show the feasibility of enhancing the catalytic ability of 2D transition metal dichalcogenide by controlling the level of defects by which a long-cycle and high-energy Li-S rechargeable battery can be achieved.

Keywords: lithium-sulfur battery, 2D material, defect, electrochemistry, catalysis

1. Introduction

Benefit from the high theoretical energy density of 2600 Wh/Kg, lithium sulfur (Li-S) batteries have been widely studied as a potential high-energy alternative for lithium ion batteries [1-4]. The total reaction of lithium sulfur battery is very complicated solid–liquid–solid phase conversion processes involving many sequential steps, in which kinetics of polysulfide conversion in the sulfur cathode is one of the most important factors to determine the final performance of lithium sulfur battery [5-8]. In particular, high sulfur loading in cathodes needed to meet high energy density outputs must demand a fast kinetical conversion of the polysulfide intermediates in the electrode reaction, which normally depends on the catalytic effect provided by the host materials of sulfur in the cathodes [9, 10].

Therefore, catalytic ability of host materials for polysulfide conversion has become one of the most concerned issues for lithium sulfur battery in the near future. Compared with the carbon-based host materials in the early research of lithium sulfur battery, transition metal composites could provide relatively high catalytic ability due to the interaction between the metal composites and polysulfides [11-14]. Transition metal dichalcogenides (TMDCs) have the characteristic sandwiched configuration of X–M–X (M, transition metal; X, chalcogen) pillared by Vander Waals forces, resulting atomic-scale thickness, direct bandgap, strong spin–orbit coupling and favourable electronic and mechanical properties [15-18]. The lamellar morphology and the good compatibility with polysulfides make TMDCs have great potential

to be used as host materials in sulfur cathodes [16, 19-21]. However, as catalytic materials, TMDCs usually provide active sites on the edge planes rather than the basal planes because the basal planes have relatively low surface Gibbs free energy and few coordination unsaturated sites [19, 22-24].

As an effective approach, introducing defects such as site vacancies and dislocations in catalytic materials can raise coordination unsaturated sites that are usually also catalytically active sites. In some cases of Li-S batteries, the vacancies in the polar configuration cause the electron coordination unsaturated to reduce electron transfer energy barrier and enhance electrophilic adsorption [25-30]. It has been demonstrated that the defects in Nb₂O₅ and MoS₂ could significantly enhance the adsorption and catalytic conversion kinetics of polysulfide intermediates [31, 32]. Moreover, acceleration of electron transport from polysulfides to electron-vacancy sites can trigger strong chemical polar-binding performance and improved catalytic kinetics [27, 33-35]. However, owing to the complicated reaction mechanism, it is actually difficult to demonstrate clearly how the defects influence Li-S batteries on electrode process and final electrochemical performance, in particular, quantitatively.

In this work, WSe_{2-x} is used as the host material in sulfur cathode on account of its merits like electronic structure of enhanced spin-orbit coupling (SOC) feature that is helpful for electron transport, compared with the other TMDCs [15, 16, 36, 37]. In WSe_{2-x}, Se vacancies are generated quantitatively by varying preparation conditions, and the site vacancies can induce the formation of dislocations in basal planes, which leads to the formation of a series of WSe_{2-x} samples with gradient Se defects. The influence of the defects on adsorption of polysulfide and catalytic effect for polysulfide conversion is investigated by theory calculations and experiments. The sample WSe_{1.51} with a moderate number of defects shows the optimal adsorption ability and catalytic ability of polysulfides. With carbon nanotubes (CNTs) as electrical connection, the S/WSe_{1.51}/CNT electrode delivers high capacity and stable cycling for Li-S batteries with a high sulfur areal loading.

2. Results and discussion

2.1 Defect regulation of tungsten selenium

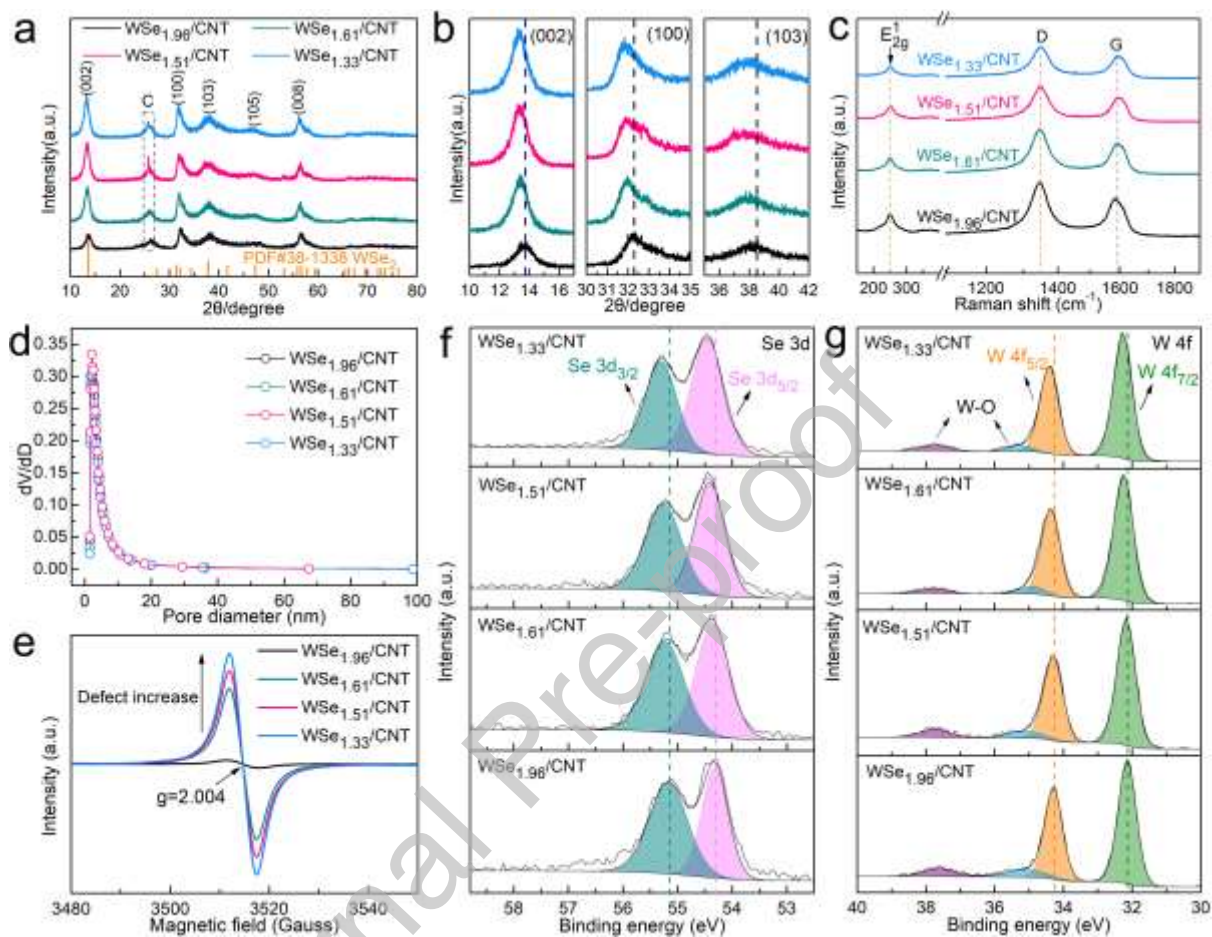


Fig. 1. Characterization of WSe_{2-x}/CNT . (a, b) XRD patterns; (c) Raman spectra; (d) Pore size distribution plots; (e) Electron spin resonance spectra; and (f, g) XPS of Se 3d and W 4f.

The solvothermal method allows to synthesize stoichiometric WSe_2 . CNTs as one-dimensional electrically conductive materials are added into the solvent to form finally the three-dimensional interlinked structure like the reported previously (Fig. S1) [38, 39]. With a little change of annealing conditions described in the experimental section, WSe_{2-x} with various amounts of Se vacancies are obtained. According to the determination results of Inductively Coupled Plasma Optical Emission Spectroscopy (ICP-OES), the ratio of W to Se for the as-prepared sample is 1.96, very close to the stoichiometric atomic ratio, and the

ratios for the three regulated samples are 1.61, 1.51, and 1.33 (Table S1), respectively, marked as $\text{WSe}_{1.96}/\text{CNT}$, $\text{WSe}_{1.61}/\text{CNT}$, $\text{WSe}_{1.51}/\text{CNT}$, and $\text{WSe}_{1.33}/\text{CNT}$. The X-ray diffraction (XRD) patterns shown in Fig. 1a confirm that all the obtained WSe_{2-x} samples have the same hexagonal structure (PDF#38-1388), and the defect regulation in the designed range has no effect on the basal crystalline phase. However, the comparison of the diffraction peaks of (002), (100) and (103) planes presents a very slight shift to low angle with the increase of defects (Fig. 1b), indicating lattice parameters enlarge marginally due to the more Se vacancies. In the Raman spectra, the peak at 250 cm^{-1} is attributed to A_1g mode of WSe_2 , and the peaks located at 1347 and 1589 cm^{-1} are the D band (disorder induced band) and G-band (graphitic band) of carbon, respectively (Fig. 1c) [20, 40, 41]. For all the samples, the peak intensity of the ratio of I_D/I_G for CNT are very close, demonstrating the defect regulation processes make no difference in the side of CNTs [42]. With increase of defects, the pore size distribution of the samples has no obvious change, but the specific surface area has light improvements from $685.1\text{ m}^2\text{ g}^{-1}$ for $\text{WSe}_{1.96}/\text{CNT}$ to $761.5\text{ m}^2\text{ g}^{-1}$ for $\text{WSe}_{1.51}/\text{CNT}$ (Fig. 1d, Table S2). The ESR results in Fig. 1e indicate clearly the gradual increase of defects from $\text{WSe}_{1.96}/\text{CNT}$ to $\text{WSe}_{1.33}/\text{CNT}$, in which the ESR signal $g=2.004$ is correlated to Se-vacancy in WSe_{2-x} , further confirming the quantitative regulation of defects [43, 44]. In addition, in the XPS results, the peaks of $\text{Se}3d$ show a gradual shift towards higher binding energy, the position of $\text{Se}3d_{5/2}$ from 54.31 eV for $\text{WSe}_{1.96}/\text{CNT}$ to 54.48 eV for $\text{WSe}_{1.33}/\text{CNT}$. This can be understood as a consequence of W-Se bonds strengthening owing to the lack of Se (Fig. 1f) [26]. Conversely, the regular shift of binding energy also confirms the gradient change of defects. The $\text{W}4f$ spectra also show consistent results, except for the two additional peaks at 35 eV and 37.6 eV derived from the inevitable surface oxidation in the XPS measurements (Fig. 1g) [26, 45].

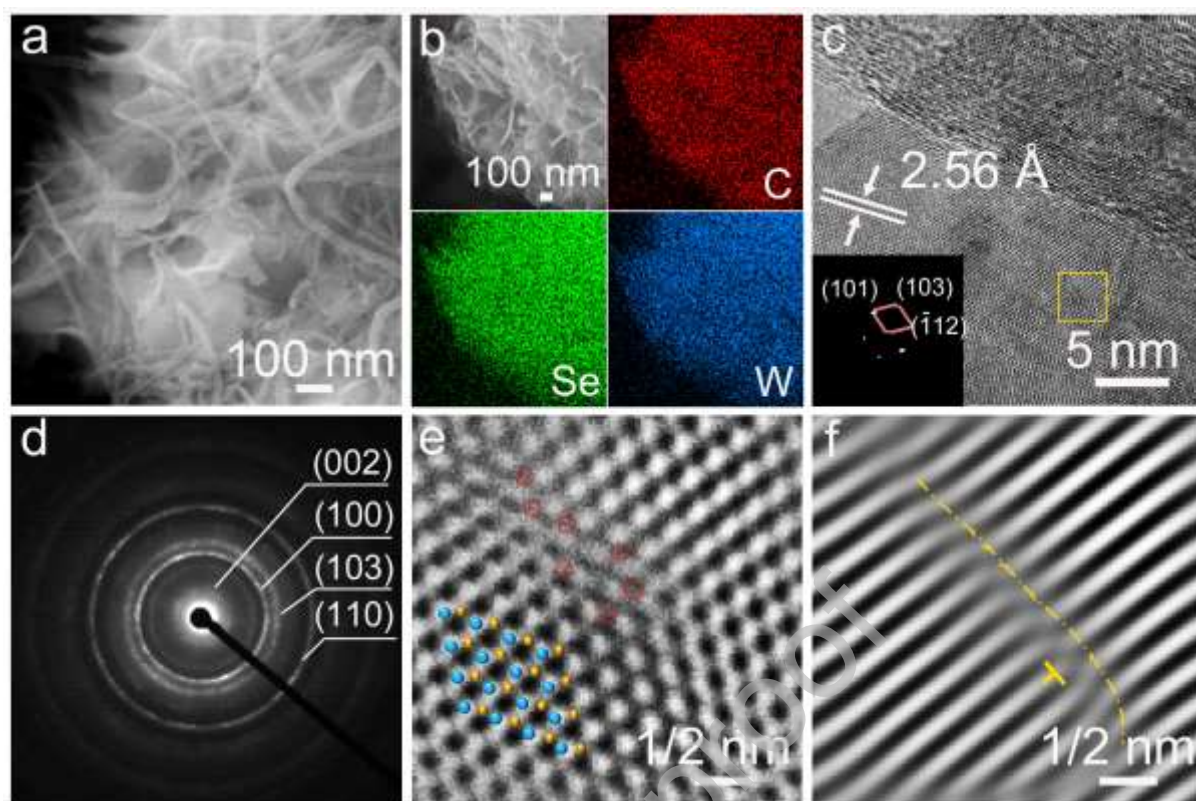


Fig. 2. Morphology and microstructure. (a) The SEM and (b) EDS elemental mapping of $\text{WSe}_{1.51}/\text{CNT}$. (c) HRTEM images of $\text{WSe}_{1.51}/\text{CNT}$ and the corresponding FFT patterns show that the prepared materials match the crystalline planes of hexagonal-phase WSe_2 (PDF#38-1388). (d) SAED image of $\text{WSe}_{1.51}/\text{CNT}$. (e, f) the IFFT pattern of the selected area by the yellow rectangle in image (c). (e, in the overlaid crystal models, blue circles represent tungsten atoms, yellow circles represent selenium atoms; red circles represent Se defect; f, yellow mark represent dislocation).

As designed, the SEM images show that 2D WSe_{2-x} and 1D CNTs can form a 3D interlinked structure which is beneficial for loading of sulfur (Fig. 2a and S2). The element mapping from energy dispersive spectroscopy (EDS) of $\text{WSe}_{1.51}/\text{CNT}$ in Fig. 2b verifies that $\text{WSe}_{1.51}$ and CNTs are homogeneously composited, and the CNTs mass content is 39.7 wt% (Fig. S3), essentially in agreement with the result determined by the elemental analysis method in Table S1 (40.47 wt%). The TEM images for all the $\text{WSe}_{2-x}/\text{CNT}$ samples clearly display 2D feature of the few-layer WSe_{2-x} and the connection between WSe_{2-x} and CNTs (Fig. S4). Influenced by the regulated vacancies, the interplanar spacing of (002) basal plane has a

gradual increase with the growing of defects (Fig. S5), consistent with the analysis of XRD results. Fig. 2c shows a typical TEM image of $\text{WSe}_{1.51}/\text{CNT}$, in which the interplanar spacing of 2.56 angstroms corresponds the (103) plane of WSe_2 , the inserted Fast Fourier Transform (FFT) pattern and the corresponding selected area electron diffraction (SAED) pattern in Fig. 2d show clearly the diffraction patterns of (002), (100), (103) and (110) planes of hexagonal WSe_2 in $\text{P6}_3/\text{mmc}$ space group. More importantly, it is found from the Inverse Fast Fourier Transform (IFFT) results based on the selected region in Fig. 2c that, besides the observable atomic point defects (Se vacancies) shown in Fig. 2e, lots of linear defects (edge dislocations) appear in the basal planes of tungsten selenide (Fig. 2f), around which there is a strain field as the atomic bonds have been compressed or stretched. For the near-stoichiometric sample $\text{WSe}_{1.96}/\text{CNT}$, few Se vacancies and edge dislocations are observed in the HRTEM analysis (Fig. S6), while plenty of defects can easily be found in the cases of $\text{WSe}_{1.61}/\text{CNT}$ and $\text{WSe}_{1.33}/\text{CNT}$ (Fig. S7 and S8).

As host materials, $\text{WSe}_{2-x}/\text{CNT}$ is loaded with sulfur by the melt diffusion method [33, 46]. In the prepared $\text{S}/\text{WSe}_{2-x}/\text{CNT}$ materials, sulfur exists as monoclinic phase (XRD, Fig. S9). The sulfur content in all the four samples are almost equal (~72 wt%), and the detailed data are determined by Thermogravimetric Analysis (TGA) shown in Fig. S10. The $\text{S}/\text{WSe}_{2-x}/\text{CNT}$ materials generally keep the original morphology of $\text{WSe}_{2-x}/\text{CNT}$ (Fig. S11), and sulfur is homogeneously distributed in the host materials (Fig. S12).

2.2 Electrochemical performance of $\text{S}/\text{WSe}_{2-x}/\text{CNT}$

In the potential range of Li-S battery (1.7~2.8 V vs Li^+/Li), the $\text{WSe}_{2-x}/\text{CNT}$ host materials are inactive and have negligible capacity contribution (Fig. S13). The batteries with $\text{S}/\text{WSe}_{1.96}/\text{CNT}$, $\text{S}/\text{WSe}_{1.61}/\text{CNT}$, $\text{S}/\text{WSe}_{1.51}/\text{CNT}$ and $\text{S}/\text{WSe}_{1.33}/\text{CNT}$ as the cathode were assembled to measure the electrochemical performances. Fig. S14 displays the CV curves of

Graphical Abstract

A little wind kindles, much puts out the fire: Controlling the level of the in-plane defects in 2D tungsten selenide enhances their catalytic ability and promote the polysulfide conversion, leading to high-performance lithium-sulfur rechargeable battery.

Quantitatively Regulating Defects of 2D Tungsten Selenide to Enhance Catalytic Ability for Polysulfide Conversion in a Lithium Sulfur Battery

